

Probing the Local Structure of Nanoscale Actinide Oxides: A Comparison between PuO_2 and ThO_2 Nanoparticles Rules out PuO_{2+x} Hypothesis

Laura Bonato,¹ Matthieu Virot,¹ Thomas Dumas,² Adel Mesbah,¹ Elodie Dalodière,¹ Oliver Dieste Blanco,³ Thierry Wiss,³ Xavier Le Goff,¹ Michael Odorico,¹ Damien Prieur,⁴ André Rossberg,⁴ Laurent Venault,² Nicolas Dacheux,¹ Philippe Moisy,² Sergey I. Nikitenko¹

¹ICSM, Univ Montpellier, CEA, CNRS, ENSCM, Marcoule, France.

²CEA, DEN, DMRC, Univ Montpellier, Marcoule, France.

³European Commission, Joint Research Centre (JRC), Institute for Transuranium Elements (ITU), Postfach 2340, 76125 Karlsruhe, Germany.

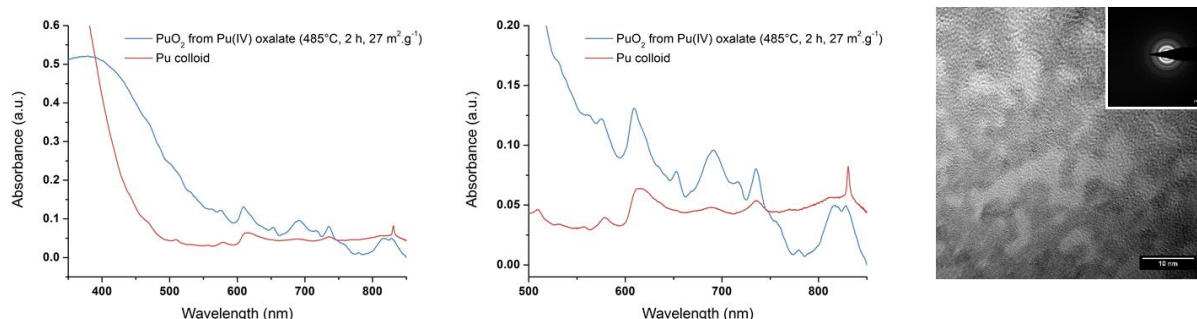
⁴Helmholtz-Zentrum Dresden - Rossendorf, Institute of Resource Ecology, Bautzner Landstraße 400, 01328 Dresden, Germany

Experimental Section

The isotopic composition (wt.%) was 96.9% ^{239}Pu , 2.99% ^{240}Pu , 0.06% ^{241}Pu ; 0.02% ^{238}Pu and 0.06% ^{242}Pu ; or 76.7% ^{239}Pu , 21.1% ^{240}Pu , 1.31% ^{241}Pu , 0.2% ^{238}Pu and 0.7% ^{242}Pu . Radiolysis was not a key-parameter to be considered within the time scale of our investigations.

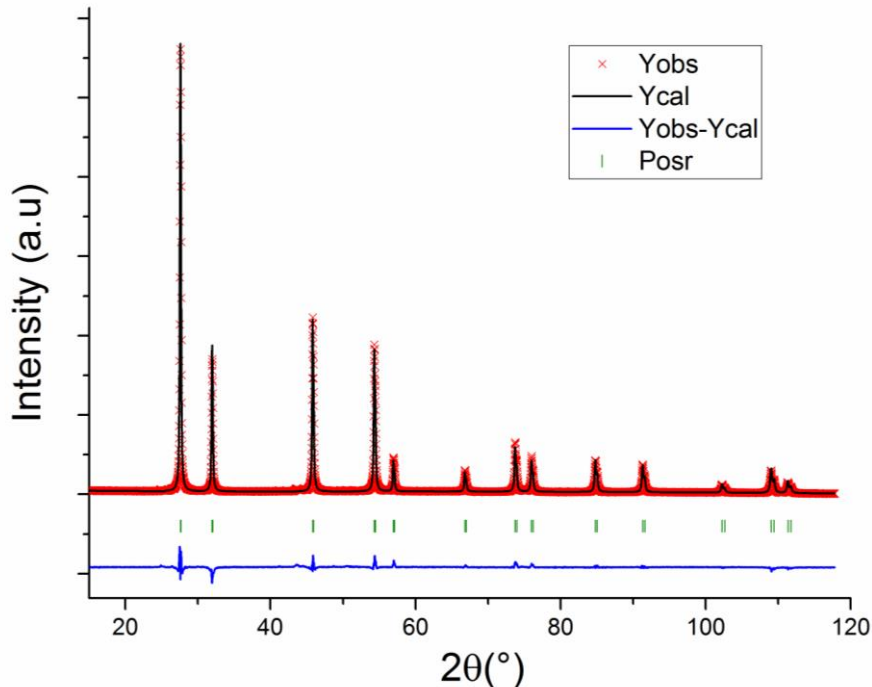
Diffuse reflectance spectroscopy

Figure S1: Diffuse reflectance spectra obtained from Pu(IV) colloid and PuO_2 (oxalic route, 485°C, 2 h). Left: comparison of both samples between 350 and 850 nm; middle: comparison of both samples between 500 and 850 nm; right: HR-TEM picture of Pu(IV) colloid evidencing the presence of spherical, monodispersed and crystalline nanoparticles. The insert is the electron diffraction pattern which agrees with PuO_2 .



XRD characterizations

Figure S2: Plot of the experimental and calculated patterns obtained on a ThO₂ sample. The difference obtained from Rietveld refinement is plotted in blue.



SEM characterizations

SEM characterizations for a selection of synthesized powders are provided in Figures S3, S4 and S5, Supporting Information. In agreement with the literature, ThO₂ powders obtained from thermal conversion of oxalate precursors are composed of polycrystalline squared-shape plate aggregates with an average length of about few hundreds nanometers to about a 1-2 micrometer(s) and a thickness of a ten to hundred nanometers.^{1, 2} The powders obtained in basic conditions (nanopowder, n-PWD) exhibit a padded and ill-defined morphology testifying the presence of very small grain aggregates. PuO₂ samples obtained from Pu(IV) oxalates also show a polycrystalline and micrometric squared-shape plate morphology whereas the oxides obtained from the conversion of Pu(III) oxalates exhibit a rod-like morphology, both method agreeing with the precursor morphology and the literature.³⁻⁶ Generally, these observations confirm that the oxides obtained by the oxalic route show a morphology preservation.⁷⁻¹⁰ The presence of very thin objects coupled to a strong porosity can nevertheless be highlighted for ThO₂ samples prepared by the oxalic route at low temperature (Figure S3) in agreement with the already reported high specific surface area (Table S1) and the low growing state of crystallites and sintered grains for such conditions (in contrast with ThO₂ powder obtained at 1000°C for instance, Figure S3).⁷

Figure S3: SEM pictures of ThO_2 samples prepared by thermal conversion of Th(IV) oxalate precursors at (a.) 485°C and (b.) 1000°C.

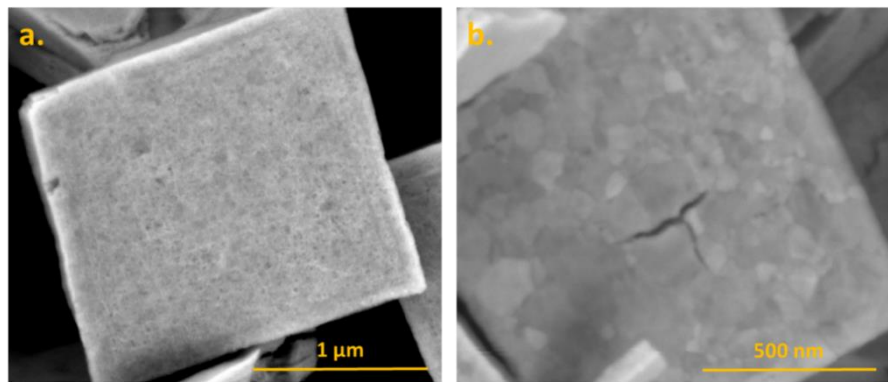


Figure S4: SEM pictures for a selection of ThO_2 samples

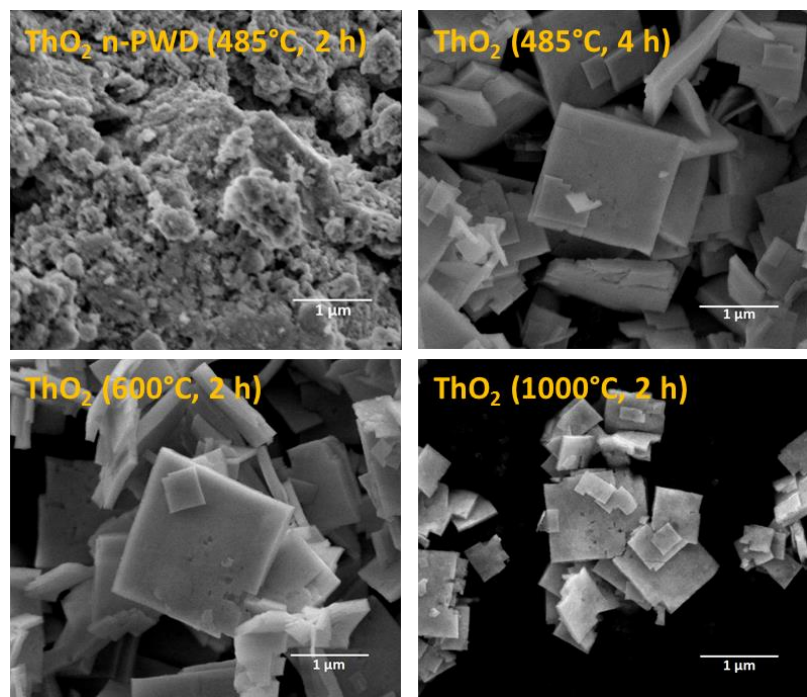
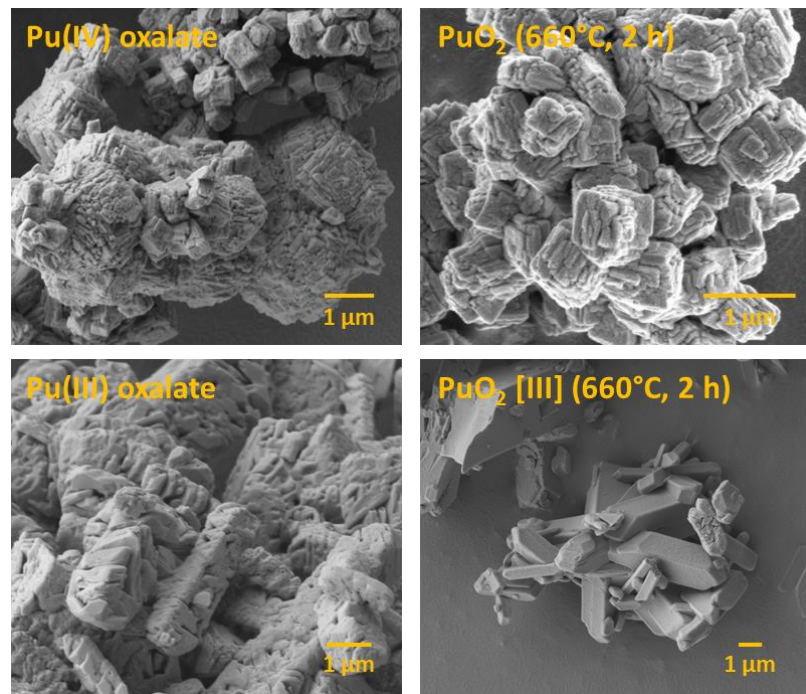


Figure S5: SEM pictures for a selection of PuO_2 samples



S_{BET} characterizations

The specific surface area of ThO_2 and PuO_2 samples (Table S1) was determined using nitrogen adsorption at 77 K after overnight degassing under vacuum at 573 K with a Micromeritics ASAP 2020 apparatus and a Micromeritics Gemini 2360 apparatus, respectively. These devices allow a limit of quantification of $\sim 1 \text{ m}^2 \text{ g}^{-1}$ and a statistical error of about 5%.

Table S1: Firing conditions used for the conversion of An(IV) precursors into ThO_2 and PuO_2 samples and their respective specific surface area measured by BET method.

Sample	Name firing temperature (duration)	Preparation route	S_{BET} ($\text{m}^2 \text{g}^{-1}$)
ThO_2	$\text{ThO}_2 485^\circ\text{C}$ (4 h)	Th(IV) oxalate	16.6
	$\text{ThO}_2 485^\circ\text{C}$ (12 h)	Th(IV) oxalate	16.4
	$\text{ThO}_2 600^\circ\text{C}$ (2 h)	Th(IV) oxalate	12.4
	$\text{ThO}_2 1000^\circ\text{C}$ (2 h)	Th(IV) oxalate	4.7
	ThO_2 n-PWD 485°C (2 h)	PEG/ammonia	-
PuO_2	$\text{PuO}_2 485^\circ\text{C}$ (2 h)	Pu(IV) oxalate	26.7
	$\text{PuO}_2 660^\circ\text{C}$ (2 h)	Pu(IV) oxalate	6.2
	$\text{PuO}_2 660^\circ\text{C}$ (17 h)	Pu(IV) oxalate	4.2
	$\text{PuO}_2 1200^\circ\text{C}$ (1 h)	Pu(IV) oxalate	< 1.2*
	PuO_2 n-PWD 485°C (2 h)	PEG/ammonia	79.2
	PuO_2 [III] 485°C (2 h)	Pu(III) oxalate	26.1
	PuO_2 [III] 485°C (12 h)	Pu(III) oxalate	20.1
	PuO_2 [III] 660°C (2 h)	Pu(III) oxalate	10.3
Pu intrinsic colloid	Pu(IV) colloid (RT)	controlled hydrolysis**	-

*value assumed from the literature describing a Pu(IV) oxalate precursor fired at 1050°C during 5 h.¹¹

**preparation conditions in agreement with our previous investigations.¹² RT: room temperature.

Figure S6: Correlation of the particle size measurements obtained by HR-TEM (measurements on the pictures) or XRD (Rietveld refinement). (a.) particle sizes lower than 25 nm; (b.) particle sizes lower than 225 nm. The red lines are the bisector functions.

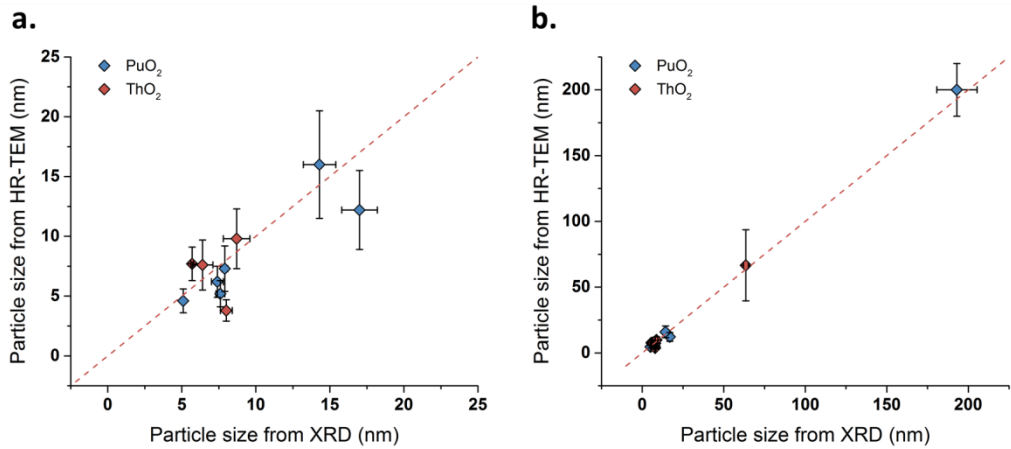


Figure S7: Raman spectra observed on ThO_2 samples annealed at different temperatures. A red-shift and FWHM increase of the T_{2g} band position is observed with the decreasing particle size composing the powders. *artefact attributed to dust on the mirror of the spectrometer. The inserts plot the FWHM and band position parameters as a function of the firing temperature.

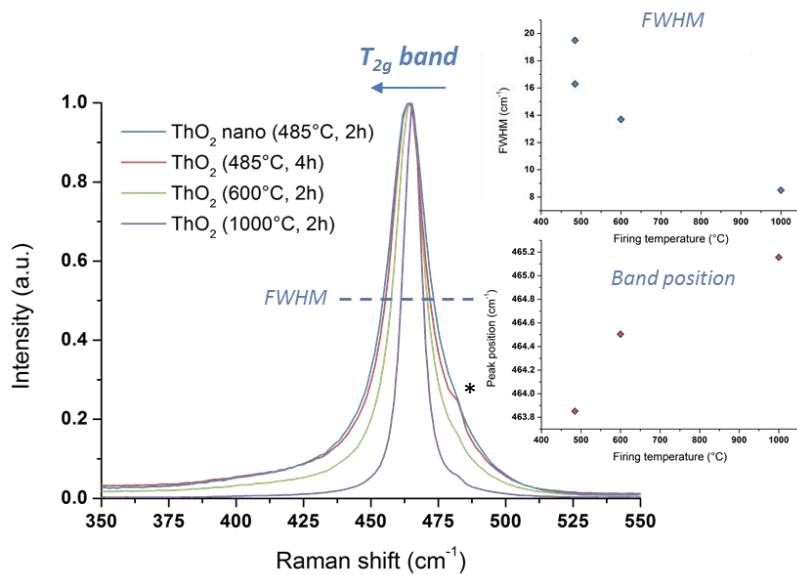


Figure S8: Normalized XANES spectra for (a., c.) ThO_2 and (b., d.) PuO_2 samples annealed at different temperatures and durations.

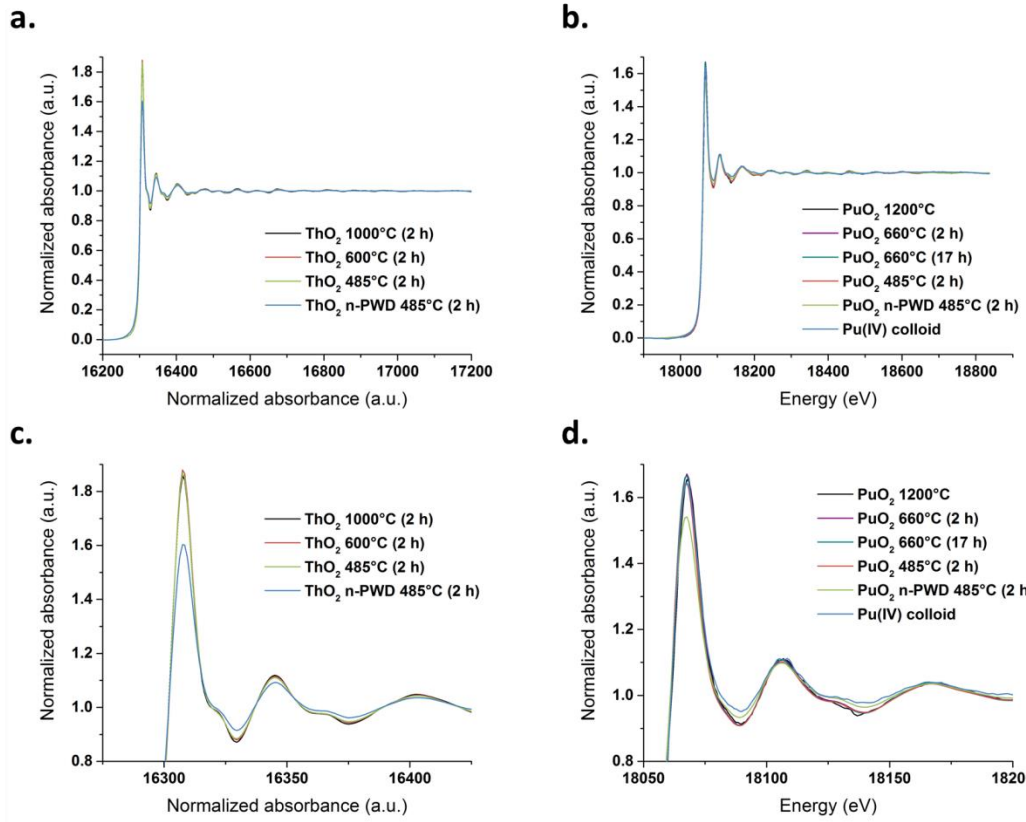


Figure S9: k^3 -weighted experimental EXAFS spectra observed for ThO_2 (left) and PuO_2 (right) samples annealed at different temperatures and durations.

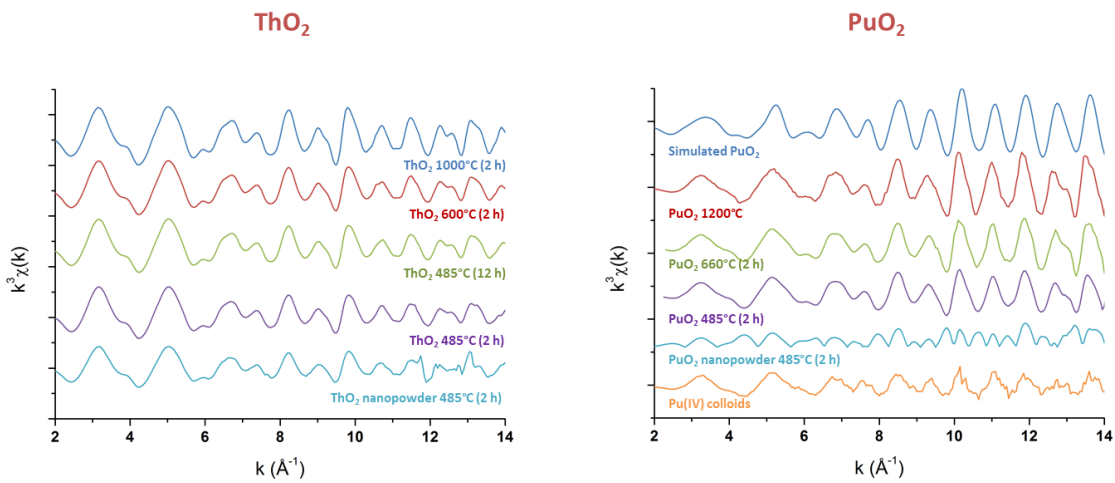


Figure S10: Fourier transform of the k³-weighted EXAFS spectra centered on the O-shell for (a.) ThO₂ and (b.) PuO₂ samples annealed at different temperatures and durations.

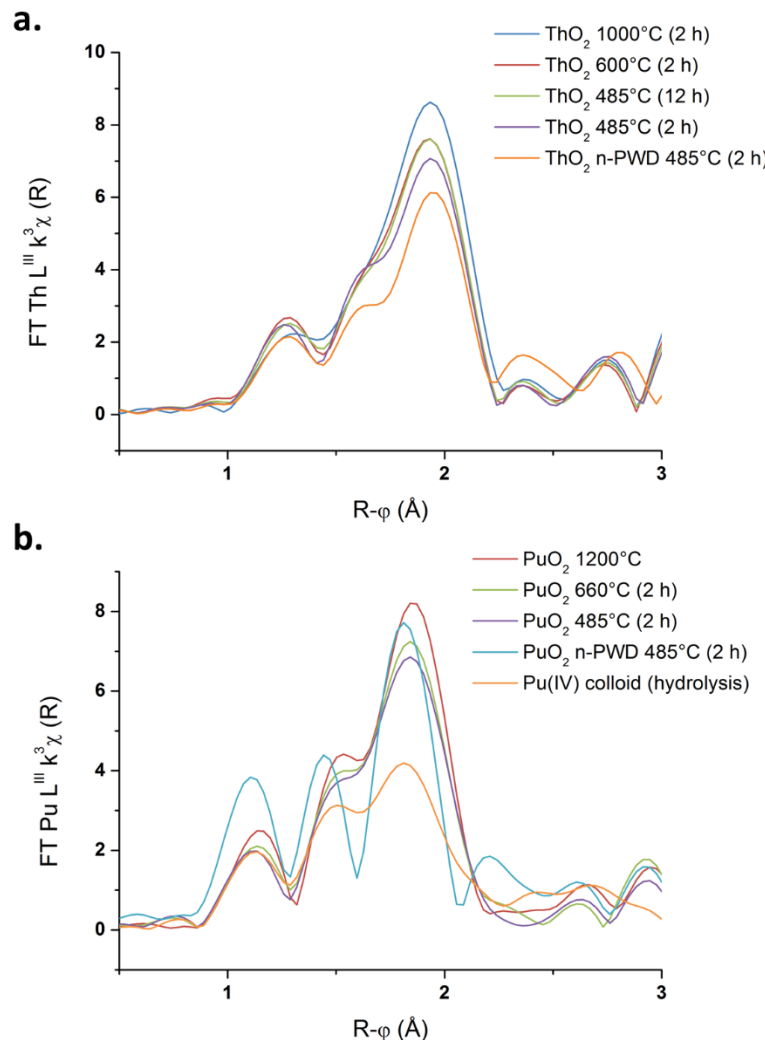


Figure S11: O-shell DWF and An-An coordination numbers for ThO_2 (a. and c., respectively) and PuO_2 (b. and d., respectively) samples as a function of the particle size determined by XRD (Rietveld refinement).

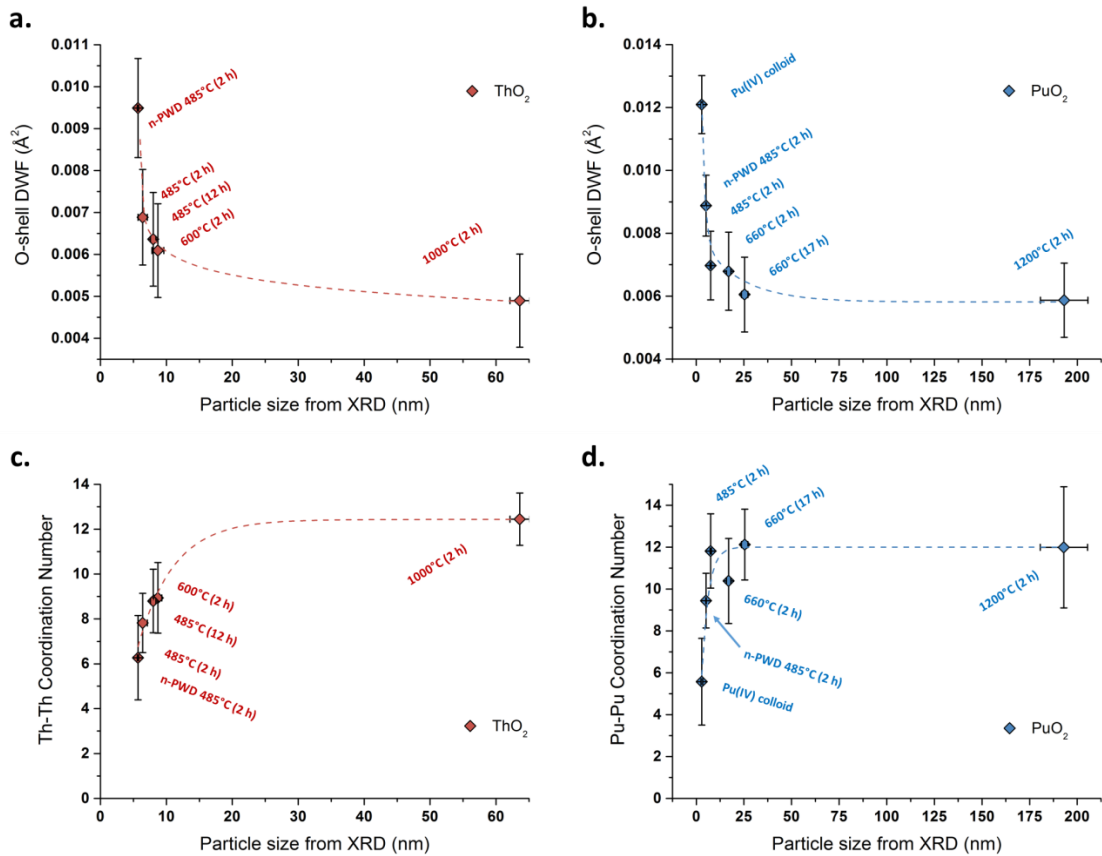
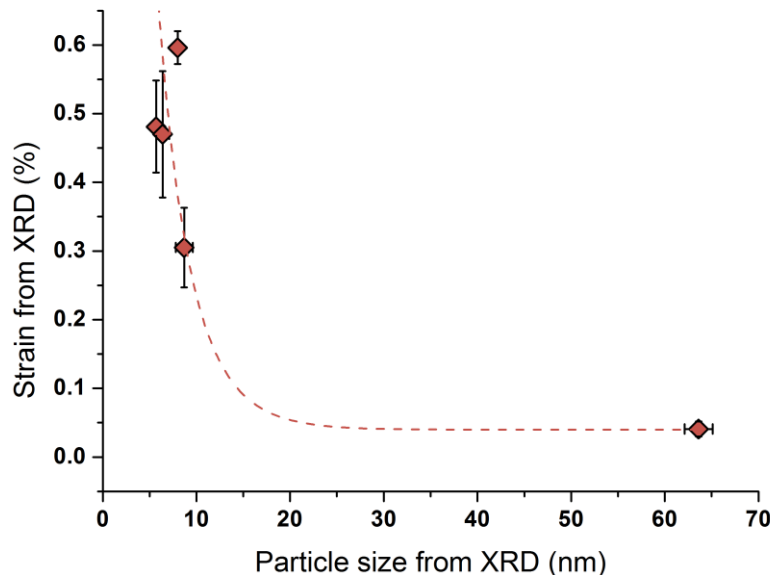


Figure S12: Strain (%) parameter as a function of ThO₂ particle size (nm) determined by XRD.



References

1. V. Tyrpekl, M. Belis, T. Wangle, J. Vleugels and M. Verwerft, *J. Nucl. Mater.*, 2017, **493**, 255-263.
2. T. Wangle, V. Tyrpekl, S. Cagno, T. Delloye, O. Larcher, T. Cardinaels, J. Vleugels and M. Verwerft, *J. Nucl. Mater.*, 2017, **495**, 128-137.
3. A.-L. Vitart, B. Haidon, B. Arab-Chapelet, M. Rivenet, I. Bisel, P. Pochon, P. Roussel, S. Grandjean and F. Abraham, *Cryst. Growth Des.*, 2017, **17**, 4715-4725.
4. L. De Almeida, S. Grandjean, N. Vigier and F. Patisson, *Eur. J. Inorg. Chem.*, 2012, DOI: 10.1002/ejic.201200469, 4986-4999.
5. R. M. Orr, H. E. Sims and R. J. Taylor, *J. Nucl. Mater.*, 2015, **465**, 756-773.
6. X. Beaudoux, M. Virot, T. Chave, G. Leturcq, G. Jouan, L. Venault, P. Moisy and S. I. Nikitenko, *Dalton Trans.*, 2016, **45**, 8802-8815.
7. V. Tyrpekl, J. F. Vigier, D. Manara, T. Wiss, O. D. Blanco and J. Somers, *J. Nucl. Mater.*, 2015, **460**, 200-208.
8. L. Claparede, N. Clavier, N. Dacheux, A. Mesbah, J. Martinez, S. Szenknect and P. Moisy, *Inorg. Chem.*, 2011, **50**, 11702-11714.
9. L. Claparede, N. Clavier, N. Dacheux, P. Moisy, R. Podor and J. Ravaux, *Inorg. Chem.*, 2011, **50**, 9059-9072.
10. D. Horlait, N. Clavier, N. Dacheux, R. Cavalier and R. Podor, *Mater. Res. Bull.*, 2012, **47**, 4017-4025.
11. X. MachuronMandard and C. Madic, *J. Alloys Compd.*, 1996, **235**, 216-224.
12. E. Dalodiere, M. Virot, V. Morosini, T. Chave, T. Dumas, C. Hennig, T. Wiss, O. D. Blanco, D. K. Shuh, T. Tyliszczak, L. Venault, P. Moisy and S. I. Nikitenko, *Sci. Rep.*, 2017, **7**.